Full article
doi.org/10.1002/elsa.202000039

Transformation to potential-program invariant form of voltammograms and dynamic electrochemical impedance spectra of surface confined redox species

Tamás Pajkossy [ORCID]

Institute of Materials and Environmental Chemistry, Research Centre for Natural Sciences, Budapest, Hungary

Correspondence

Tamás Pajkossy, Institute of Materials and Environmental Chemistry, Research Centre for Natural Sciences, Magyar tudósok körútja 2, Budapest, Hungary, H-1117. Email: pajkossy.tamas@ttk.hu

Abstract

A theory is presented by which voltammograms, and dynamic electrochemical impedance spectroscopy (dEIS) measurements of redox processes of surface-confined species can be analyzed. By the proposed procedure, from a set of voltammograms taken at varied scan-rates, two scan-rate independent, hysteresis-free functions of potential can be calculated. One of them characterizes the redox kinetics, the other is the electrode charge associated with the redox equilibrium. The theory also comprises the analysis of the impedance spectra of the same system, which have been measured during dynamic conditions, i.e., during potental scans. Because of the formal analogy, the procedure is applicable also for voltammetry and dEIS of adsorption processes.

KEYWORDS
charge transfer, data analysis, electrode, kinetics

1 | INTRODUCTION

Cyclic voltammograms, CVs, are usually complicated functions of the scan-rate; they often exhibit large hysteresis. Comparison of two CVs measured with different scan-rates is far from being trivial. The comparison is even more complicated if the scan-rate varies in time or when two voltammograms are measured with different, arbitrary waveforms of potential program – this form of voltammetry will be denoted hereafter as arbitrary waveform voltammetry, AWV.

In rare, simple cases, however, there exist mathematical transformations by which AWVs taken with different potential programs (e.g., CVs with different scan-rates) can be transformed to the one-and-the-same potential-program invariant (PPI) function – which function is

independent of the actual form of the potential-time function. For example, the CVs of reversible redox couples – whose both forms are soluble – can be transformed to hysteresis-free sigmoid-shaped curves using semiintegration.[1] In contrast, the AWVs of redox systems of slower kinetics – of the so-called quasi-reversible systems – cannot be transformed to a single PPI function. However, as it has recently been demonstrated in ref. [2], by measuring a set of quasi-reversible AWVs with varied scan-rates, two PPI functions can be obtained by a simple numerical procedure. One of them characterizes charge transfer kinetics, the other diffusion.

The same electrochemical system can be studied also by analyzing the electrochemical impedance spectra (EIS) yielding two elements of the Faradaic impedance: charge transfer resistance and the coupled Warburg-coefficient at

Electrochem. Sci. Adv. 2021;e2000039.   wileyonlinelibrary.com/journal/elsa   **1 of 11**

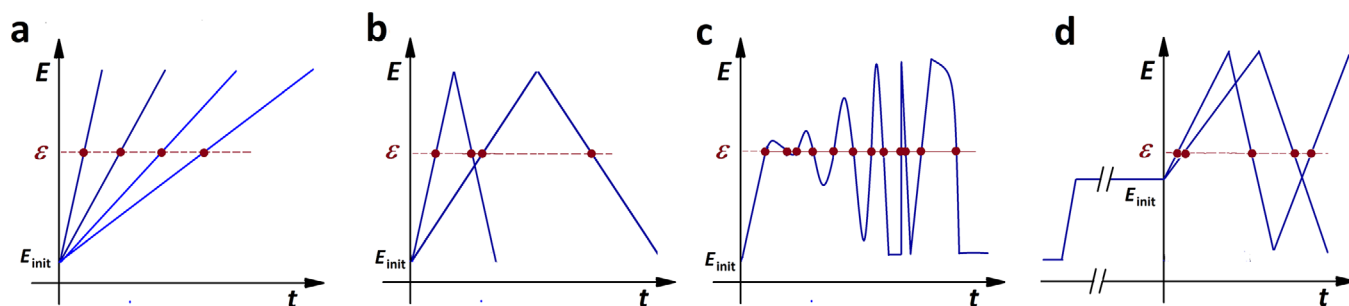https://doi.org/10.1002/elsa.202000039

FIGURE 1 $E(t)$ of typical experiments for which the theory applies. (a) Single scan experiments with varied scan-rates. (b) CVs of varied scan-rates. (c) Voltammograms with arbitrary $E(t)$, performed with any electric (potentiostatic, galvanostatic, or mixed) control. (d) Voltammetry when E_{init} is in the peak-potential range (case analyzed in the Appendix)

a given potential. The same applies also to dEIS (dynamic EIS) measurements, when high-frequency impedance spectra are measured while the potential is scanned to simultaneously accomplish CV or AWV measurements. In case of dEIS, both the charge transfer resistance and the Warburg coefficient depend on the applied potential program, e.g., on scan-rate. To eliminate the potential program dependence, a procedure has been presented [3] yielding two PPI functions. These are closely related to the EIS results, and also to the PPI functions which are the transformed forms of the AWVs.

Here, we present the analysis of another important electrochemical situation: when the rate of the electrode process is limited by the finite quantity of the reactants. We have recently derived the transformations yielding PPI functions for the case of adsorption-desorption of charged species on an electrode surface with a finite density of adsorption sites [4]. As it already has been alluded therein, the AWVs and dEIS of redox reactions of surface-confined species can be treated analogously. This is the subject of the present paper.

2 | THEORY

2.1 | Voltammetry

Consider a metal-electrolyte interface where both forms, Red and Ox, of some redox species, A, are bound to the electrode surface. They can be transformed to each other in the n-electron transfer reaction $\mathrm{Red}_s^{z+} \rightleftharpoons \mathrm{Ox}_s^{(z+n)+} + n\mathrm{e}^-$; this is called as a redox reaction of surface-confined species. Let the interfacial density of the oxidized and reduced forms be denoted by Γ_{ox} and Γ_{red} (in mol/cm^2 unit) whereas their sum, the total interfacial density of the two forms is Γ_A. The $\theta = \Gamma_{ox}/\Gamma_A$ ratio will be named as the coverage of the oxidized state; the standard potential of the redox system – at which, in equilibrium, $\Gamma_{ox} = \Gamma_{red}$ – will be denoted as E_0.

We perform a voltammetry experiment, that is, we measure the current density, j as a function of potential, E, which varies in time, t. For the sake of simplicity, we will use the term AWV for this experiment, since it can be performed not only with regular triangular but with any arbitrary waveforms, of time-varying scan rate $v \equiv \mathrm{d}E/\mathrm{d}t$. The potential changes according to a program crossing the $E = \varepsilon$ level more than once during the experiment; its possible ways – repetitive one-way or cyclic scans with varied scan rates, or one continuous back-and-forth cycle-series with varied scan-rates and vertex potentials - are illustrated in Figure 1. Prior to the potential program (or scans as in case a), the electrode is assumed to be in a steady state at potential E_{init}, where the electrode charge is q_{init}. In this Section, we consider the simple case when E_{init} is sufficiently negative to be out of the redox peak potential range. The general case of starting the experiment at any value of E_{init} is analysed in an Appendix.

In what follows, we analyze the rate equations by adhering to the usual theorization of electrochemical kinetics [5] but ignore the complication factors of IR drop and double-layer charging. However, these complicating issues will be shortly considered in the Discussion.

As double layer charging is out of our present scope, the current density j is always the time derivative of the electrode charge density q, i.e. the charge density of redox species bound to the electrode surface. At any time instance t,

$$j(t) = dq(t)/dt = \partial q/\partial\Gamma_{red} \cdot d\Gamma_{red}/dt$$
$$+ \partial q/\partial\Gamma_{ox} \cdot d\Gamma_{ox}/dt = n\mathrm{F} \cdot d\Gamma_{ox}/dt \qquad (1)$$

where F is the Faraday constant. By integrating Equation 1 with respect to time, we get

$$q(t) = \int_0^t j(\tau)\,\mathrm{d}\tau = n\mathrm{F} \cdot \Gamma_{ox}(t) - q_{init} \qquad (2)$$

3 of 11 **Electrochemical Science Advances** Full article
doi.org/10.1002/elsa.202000039

**Chemistry
Europe**
European Chemical
Societies Publishing

The net rate of redox process, assuming the simplest first-order kinetics, is written as

$$d\Gamma_{ox}(t)/dt = k_{ox}(E) \cdot \Gamma_{red}(t) - k_{red}(E) \cdot \Gamma_{ox}(t) \quad (3)$$

where k_{ox} and k_{red} are the rate coefficients of oxidation and reduction, respectively. Note that only the rate coefficients depend on E, in a yet unspecified way; the time dependence of j stems from that of the Γ surface concentrations.

With the introduction of the

$$H(E) = k_{ox}(E) + k_{red}(E) \quad (4)$$

variable, by combining Equations (1) to (3) we get

$$j(t) = nF \cdot \Gamma_A \cdot k_{ox}(E) - H(E) \cdot q_{init} - H(E) \cdot q(t) \quad (5)$$

Eq. (5) applies for any $j(t)$ vs $q(t)$ plot. As mentioned above, in what follows, the potential program is assumed to start at time $t = 0$ from a sufficiently negative value of E_{init} where the surface confined redox species is fully reduced; i.e. at $E_{init} \ll E_0$, $q_{init} = 0$. If we have a number of $j(t)$ vs $E(t)$ plots, for all data points – measured at time instance τ with $E = \varepsilon$, the

$$j(\tau) = nF \cdot \Gamma_A \cdot k_{ox}(\varepsilon) - H(\varepsilon) \cdot q(\tau) \quad (6)$$

equation holds. That is, if we measure a voltammogram which crosses some potential ε at least two times, then all the j vs q points of the same ε potential appear on one and the same $j = const_1 - const_2 \cdot q$ line. This is shown in Figure 2, as a dashed line. With increasingly positive scan-rate, the points move toward the ordinate; the physical meaning of the ordinate intersect, $const_1$ is the oxidation rate – expressed as current density – as if the complete surface were completely reduced, $\Gamma_{ox} = 0$. Technically, we get these points when q is little: if, for a given k_{ox}, only a short time has passed since time zero. It is the case when the experiment is carried out as fast ("infinitely" fast) as to keep q close to zero. This is why it will be denoted as j_{inf}. Thus,

$$j_{inf}(\varepsilon) = nF \cdot \Gamma_A \cdot k_{ox}(\varepsilon) \quad (7)$$

Equation (6) now reads as

$$j(\tau) = j_{inf}(\varepsilon) - H(\varepsilon) \cdot q(\tau) \quad (8)$$

The physical meaning of the abscissa intercept is the surface charge acquired by oxidation in a long time. As $j = 0$, the anodic and cathodic currents are equal, the system is kinetically reversible. Technically, we get these points on –or, in the close vicinity of – the abscissa, when k_{ox} is very
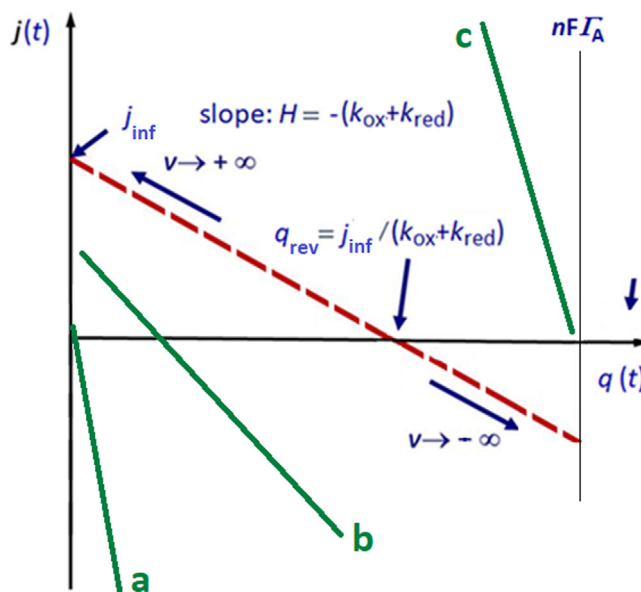

FIGURE 2 The dashed line and annotations illustrate the quantities of Equations (7–9). The solid lines a, b, and c are characteristic to potentials negative to the redox peak, under the peak, and at positive potentials, respectively

high and/or the experiment is carried out very slowly, a steady state is attained. Hence the abscissa intersect will be denoted as q_{rev}; therefore Equation (8) can be rearranged to yield the following form:

$$q(\tau) = q_{rev}(\varepsilon) - j(\tau)/H(\varepsilon) \quad (9)$$

From Equations (8) and (9) two simple equations emerge:

$$H(\varepsilon) = j_{inf}(\varepsilon)/q_{rev}(\varepsilon) \quad (10)$$

and

$$j(\tau)/j_{inf}(\varepsilon) + q(\tau)/q_{rev}(\varepsilon) = 1 \quad (11)$$

Equations (8) and (9) are the key equations using which we can get j_{inf} and q_{rev} as a function of potential. As they depend on potential only, they do not depend on the scan-rate, moreover the actual shape of the potential program, by which the js have been measured. In the same vein, since they are single-valued functions, the j vs q curves do not exhibit any hystereses.

Equations (8) to (11) connect j and q values at one and the same ε potentials. As ε may have any value, in what follows, the parameters of these equations will be functions of E. According to the above equations, for infinitely slow, kinetically irreversible reactions all points of the $j(t)$ vs $q(t)$ plot, lie on the j axis, in the complete potential range. For kinetically reversible processes all points are on the q axis.

The quasi-reversible reactions are the ones for which tilted lines appear on that plot.

The $H(E) = k_{ox}(E) + k_{red}(E) = j_{inf}(E)/q_{rev}(E)$ equation is of central importance in coupling aspects of kinetics and thermodynamics. This is valid for any form of potential dependence defined for the k_{ox} and k_{red} rate coefficients. However, assuming exponential potential dependences of the rate coefficients is usual in the electrochemical kinetics theories in general, and in the case of surface confined reactions in particular[6,7]). That is, the rate coefficients are of the form of $k_{ox}(E) = k_{ox}^0 \cdot \exp(\alpha_{ox}FE/RT)$ and $k_{red}(E) = k_{red}^0 \cdot \exp(-\alpha_{red}FE/RT)$ where the symbols have their usual meaning. With these exponential dependences Equation (7) gets the following form:

$$j_{inf}(E) = nF \cdot \Gamma_A \cdot k_{ox}^0 \cdot \exp(\alpha_{ox}FE/RT) \qquad (12)$$

and as $q_{rev}(E) = j_{inf}(E)/H(E)$ (cf. Equation (10)),

$$q_{rev}(E) = \frac{nF \cdot \Gamma_A \cdot k_{ox}^0 \exp(\alpha_{ox}FE/RT)}{k_{ox}^0 \exp(\alpha_{ox}FE/RT) + k_{red}^0 \exp(-\alpha_{red}FE/RT)}$$

$$= \frac{nF \cdot \Gamma_A}{1 + k_{red}^0/k_{ox}^0 \exp(-(\alpha_{ox} + \alpha_{red})FE/RT)} \qquad (13)$$

By defining $E_0 = RT/[(\alpha_{ox} + \alpha_{red})F] \cdot \ln(k_{red}^0/k_{ox}^0)$ as a standard potential, and assuming $\alpha_{ox} + \alpha_{red} = n$, we get

$$q_{rev}(E) = \frac{nF \cdot \Gamma_A}{1 + \exp(-nF(E - E_0)/RT)}$$

$$= (nF \cdot \Gamma_A/2) \cdot [1 + \tanh(nF(E - E_0)/RT)] \qquad (14)$$

or in another, Nernst-equation-like format

$$E = E_0 + \frac{RT}{nF} \ln\left[\frac{q_{rev}(E)}{nF \cdot \Gamma_A - q_{rev}(E)}\right] \qquad (15)$$

Equations (14) and (15) are the algebraic forms of the well-known sigmoid curves frequently showing up in electrode kinetics in various contexts (e.g., as the functional form of the polarographic waves).

2.2 | Dynamic electrochemical impedance spectroscopy

Consider the same system and measurement as in the previous section, but the potential program comprises also a high frequency, low amplitude sinusoidal perturbation of angular frequency ω upon the top of a slow poten-

tial scan. In other words, the potential program is a sum of a quasi-dc and of an ac term; the ac perturbation is used for the measurement of impedance. We assume that the temporal change rates of the dc and ac voltages differ much, hence the steady state – the basic condition of measuring impedance spectra – at least approximately applies. In what follows, we calculate the impedance function of this system. The perturbed quantities, $x_p(t)$, (any of j, E, and q) are of the form $x_p(t) = x(t) + \overline{x_{ac}}\exp(i\omega t)$ where i is the imaginary unit, and the overlining refers to a complex amplitude. For brevity, this form will be abbreviated as $x_p(t) = x(t) + \delta x$. Since the potential perturbation amplitude is assumed to be low, we may apply the usual assumption that no superharmonics are generated. Accordingly, the $y_p(E)$ quantities with a perturbation (the $k(E)$ rate coefficients, and $H(E)$) can be expanded to a series and the higher order terms can be dropped, yielding formulae $y_p(E_p(t)) = \cdot y(E) + dy/dE \cdot \overline{E_{ac}} \cdot \exp(i\omega t) = y + \delta y$. This way Equation (6) is written as

$$j(t) + \delta \mathbf{j} = nF \cdot \Gamma_A \cdot (k_{ox} + \delta k_{ox})$$
$$- (H + \delta \mathbf{H}) \cdot (q(t) + \delta \mathbf{q}) \qquad (16)$$

The dc terms cancel each other (cf. Equation (6)), for the remaining ac terms of ω frequency we get

$$\delta \mathbf{j} = nF \cdot \Gamma_A \cdot \delta k_{ox} - q(t) \cdot \delta \mathbf{H} - H \cdot \delta \mathbf{q} \qquad (17)$$

with $\delta k_{ox} \equiv dk_{ox}/dE \cdot \overline{E_{ac}} \cdot \exp(i\omega t)$, and $\delta H \equiv dH/dE \cdot \overline{E_{ac}} \cdot \exp(i\omega t)$, we obtain

$$\overline{j_{ac}} = nF \cdot \Gamma_A \cdot \mathbf{d}k_{ox}/\mathbf{d}E \cdot \overline{E_{ac}}$$
$$- H \cdot \overline{q_{ac}} - q(t) \cdot \mathbf{d}H/dE \cdot \overline{E_{ac}} \qquad (18)$$

Taking into account the integral relation of q and j, i.e. $\overline{q_{ac}} = \overline{j_{ac}}/(i\omega)$; introducing j_{inf} as defined by Equation (7), we get

$$Z(\omega) \equiv \overline{E_{ac}}/\overline{j_{ac}} = \left(1 + \frac{H}{i\omega}\right) / \left(\frac{dj_{inf}}{dE} - \frac{dH}{dE}q(t)\right) \qquad (19)$$

Equation (19) expresses the impedance of a charge transfer resistance, R_{ct}, and an associated pseudocapacitance, C_{ct} connected serially. These elements are as follows:

$$\frac{1}{R_{ct}(E)} = \frac{dj_{inf}}{dE} - \frac{dH}{dE}q(t) \qquad (20)$$

$$C_{ct}(E) = \frac{1}{H} \cdot \left(\frac{dj_{inf}}{dE} - \frac{dH}{dE}q(t)\right) \qquad (21)$$

Two points are noteworthy: First, the product of Equations (20) and (21) reveals that R_{ct} and C_{ct} are coupled, through the coupling constant $1/H(E)$:

$$C_{ct}(E) \cdot R_{ct}(E) = 1/H(E) \qquad (22)$$

Second, for $1/R_{ct}$ and C_{ct} both, a $const_1 - const_2 \times q$ type equation applies where the constants are related also to the constants of the dc relations. Equations (20) and (21) are equations by which the information on kinetics can be extracted from the Faradaic impedance data.

To extract the surface charge, i.e., the thermodynamic data, Equations (20) and (21) are to be changed to show the impedance elements vs $j(t)$ connection. To this, we substitute $q(t)$ by $j(t)$ using Equation (9), and j_{inf} by q_{rev} using Equation (10). Equations (20) and (21) can be re-written to yield R_{ct} vs j and C_{ct} vs j equations as follows:

$$\frac{1}{R_{ct}(E)} = \frac{dj_{inf}}{dE} - \frac{dH}{dE}q(t) = \frac{dj_{inf}}{dE} - \frac{dH}{dE}\left(q_{rev} - \frac{j(t)}{H}\right)$$

$$= H \cdot \frac{dq_{rev}}{dE} + \frac{1}{H} \cdot \frac{dH}{dE}j(t) \qquad (23)$$

$$C_{ct}(E) = \frac{1}{H \cdot R_{ct}(E)} = \frac{dq_{rev}}{dE} + \frac{1}{H^2} \cdot \frac{dH}{dE}j(t) \qquad (24)$$

It is worth to define $R_{ct,inf} \equiv 1/(dj_{inf}/dE)$ and $C_{ct,rev} \equiv dq_{rev}/dE$ with these denotions Equations (20) and (24) read as

$$\frac{1}{R_{ct}(E)} = \frac{1}{R_{ct,inf}} - \frac{dH}{dE}q(t) \qquad (25)$$

and

$$C_{ct}(E) = C_{ct,rev} - \frac{d(1/H)}{dE}j(t) \qquad (26)$$

Equations (20) to (24) are the key equations using which we can get $1/R_{ct,inf}$ and $C_{ct,rev}$ as a function of potential. Three points are to be emphasized here:

a. Just as j_{inf} and q_{rev} in the case of voltammetry, $1/R_{ct,inf}$ and $C_{ct,rev}$ are PPI invariant functions.
b. Just as in voltammetry, the $H(E) = 1/(C_{ct}(E) \cdot R_{ct}(E))$ quantity is the coupling quantity of kinetics and thermodynamics. However, in this case, $H(E)$ connects the directly measured impedance parameters rather than the extrapolated currents and charges.
c. Note that in the usual, steady-state EIS measurements – as no steady-state Faraday-current flows in such a system, $j(t) = 0$, hence then, $C_{ct}(E)$ is the potential

derivative of q_{rev} (cf. Equation (24)). Just as in dEIS, information on kinetics can be obtained using Equation (22), directly from $R_{ct}(E)$ and $C_{ct}(E)$.

2.3 | Common features of the PPI functions

Summarizing the findings of Sections 2.1 and 2.2, we present a table with the connections of the relevant quantities. In Table 1, the linear dependences connecting the four important measured quantities (j, q, R_{ct}, C_{ct}) with the four PPI quantities (j_{inf}, q_{ox}^{eq}, dj_{inf}/dE, dq_{ox}^{eq}/dE) are summarized.

These equations have been derived with the assumption that $q_{init} = 0$. As it is demonstrated in the Appendix, if $q_{init} > 0$; the linear equations of Table 1 still hold with unchanged slopes but with changed intercepts. The consequences are discussed therein with the practical conclusion that both for the understanding and for performing data analysis the above theory is just sufficient.

3 | DISCUSSION

3.1 | Numerical illustration of the transformation yielding the PPI form

Although the derivation presented in the Theory section is simple and straightforward, it is instructive to show how to perform the calculation by which from AWVs can be transformed to PPI form. First, based on Equations (1) to (3), four CVs have been simulated with different scan rates. Just as described in the context of Equations (12)-(15) for the rate coefficients exponential dependences on potential were assumed. The simulation parameters were as follows: $\alpha_{ox} = 0.3$, $\alpha_{red} = 0.7$, $n = 1$, $k_{ox}^0 = k_{red}^0 = 1 \text{ s}^{-1}$, $\Gamma_A = 2 \times 10^{-9}$ mol/cm^2. These CVs, for visibility reasons normalized by the scan-rate, are displayed in Figure 3a; they are rather similar to the ones in the literature (cf. Figure 4 of [6] and Figure 2 of [7], the slight differences are due to the asymmetry of the α transfer coefficients).

The steps of the procedure of getting the PPI forms are as follows: First, the integrated forms are calculated (see Figure 3b). As it is shown in Figure 3c for a couple of potentials, the $j - q$ dependence is linear. According to Eq. (8), straight lines were fitted to each set of $j - q$ points by a linear least squares program. Finally, from the fitted slopes and intercepts j_{inf} and q_{rev} values were calculated for each potential; these are shown in Figure 3d. Both curves are hysteresis-free; the $lg(j_{inf})$ vs E is a straight

6 of 11　　**Electrochemical Science Advances**　　Full article
doi.org/10.1002/elsa.202000039

Chemistry
Europe

European Chemical
Societies Publishing

TABLE 1　The linear dependencies. Note the reciprocal symmetries of the slopes

Equation No.	Dependence	Intercept	Slope
(8)	$j(t)$ vs $q(t)$	j_{inf}	$-H$
(20)	$1/R_{ct}$ vs $q(t)$	$\dfrac{dj_{inf}}{dE} \left[\equiv \dfrac{1}{R_{ct,inf}}\right]$	$-\dfrac{dH}{dE}$
(21)	C_{ct} vs $q(t)$	$\dfrac{1}{H} \cdot \dfrac{dj_{inf}}{dE}$	$\dfrac{-1}{H} \cdot \dfrac{dH}{dE}$
(9)	$q(t)$ vs $j(t)$	q_{rev}	$-1/H$
(24,26)	C_{ct} vs $j(t)$	$\dfrac{dq_{rev}}{dE} \left[\equiv C_{ct,rev}\right]$	$-\dfrac{d(1/H)}{dE}$
(23,25)	$1/R_{ct}$ vs $j(t)$	$H \cdot \dfrac{dq_{rev}}{dE}$	$+\dfrac{1}{H} \cdot \dfrac{dH}{dE} \left[= -\dfrac{1}{1/H} \cdot \dfrac{d(1/H)}{dE}\right]$
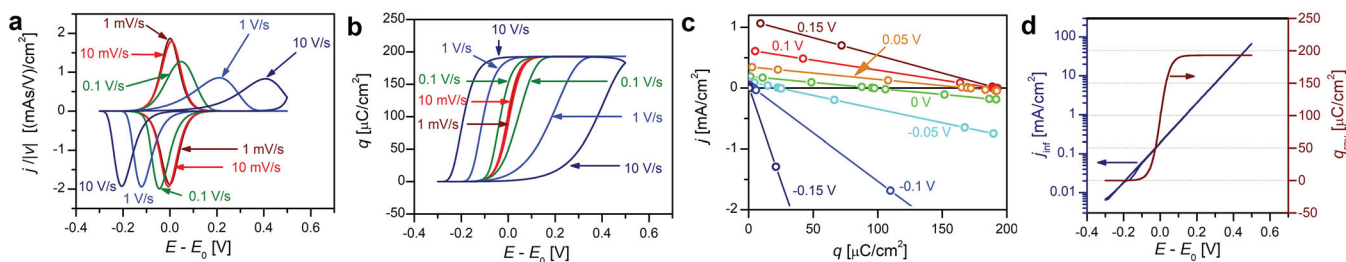
FIGURE 3　Simulated CVs of surface confined redox systems, and the procedure of calculation of the PPI representation. (a) The calculated scan-rate normalized CVs at scan-rates as indicated; (b) The integrated CVs; (c) The linear connection of j and q at potentials as indicated; (d) j_{inf} and q_{rev} as a function of potential

line, the q_{rev} vs E is a sigmoid shape (tanh) function, as predicted by Equations (12) and (14), respectively. The characteristic values of the curves: j_{inf}, q_{rev} and the $d\log(j_{inf})/dE$ slope at $E = 0$ are exactly the same as the ones which can be calculated from the input data.

In general, Equations (8) and (9) hold without any constraint to the specific form of potential dependence of the rate coefficients. Accordingly, other than exponential $k_{ox}(E)$ and $k_{red}(E)$ functions also lead to the two PPI functions, as it is demonstrated in Figure 4. For simulating the CVs of Figure 4a, we assumed rate coefficients with power-law potential dependences (though such a dependence is highly unusual and irrealistic in electrochemical kinetics). This way the rate coefficients are $k_{ox}(E) = const_1 \cdot (E - E_1)^4$ and $k_{red}(E) = const_1 \cdot (E - E_1)^{-4}$ with $E_1 = -0.4 \, [V]$. As it is seen in Figure 4b, both $j_{inf}(E)$ and $q_{rev}(E)$ are hysteresis-free. The $\lg(j_{inf})$ vs $\lg(E - E_1)$ plot is a straight line with a slope of 4, in accord with $j_{inf}(E) \propto k_{ox}(E) \propto (E - E_1)^4$.

3.2 | General comments

Apparently Equations (8) to (11) are trivial combinations of three well-known, basic equations of physical chemistry. The novelty of the theory of this paper is that we

do not attempt to calculate the $j(E)$ function of a single CV as it was done by in the previous studies employing exponential potential dependences for the rate coefficients [6,7]. Instead, we set aside the potential dependence of the rate coefficients and evaluate a set of AWVs with different scan-rates together at the same potential. This is how we can extrapolate to standard surface conditions of kinetics and redox equilibrium at a certain potential. Another novelty is the calculation of the PPI forms of both of the large and small-signal response functions (AWV and dEIS, respectively) and demonstrating their functional connections. Hence this derivation – just as the results – are analogous to those of the quasireversible diffusion-controlled redox reaction case of refs. [2] and [3].

There is another analogy: the theory of the present paper with little terminology changes applies also for adsorption processes. A preliminary version of such a theory is the one in Ref. [4] – which lead to equations similar to those of the present Equations (8) to (10); however, it contained neither the impedance analysis part, nor the derivation of the present Appendix. The present theory, *mutatis mutandis*, can be simply used for the analysis of adsorption-related AWV and dEIS measurement results. The most important conceptual changes to be done are the replacement of $k_{ox}(E)$ to $c \cdot k_{ad}(E)$, $k_{red}(E)$ to $k_d(E)$ and n to γ (where c is the adsorbate concentration and γ is the formal partial charge number [8]).
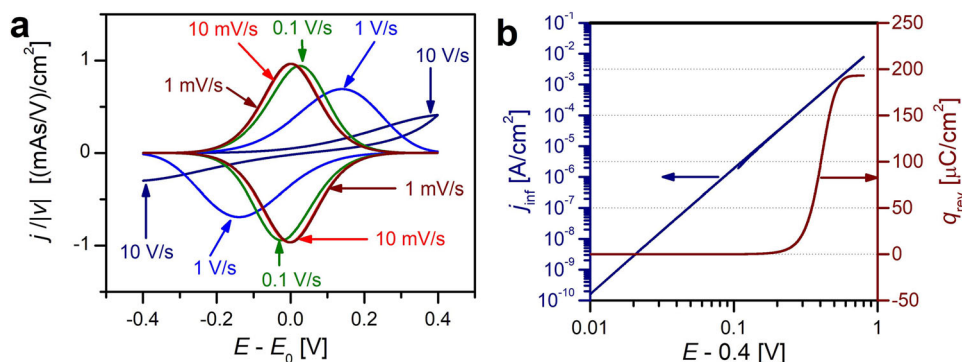
FIGURE 4 (A) CVs generated with a power-law function of the potential and (B) their PPI form

TABLE 2 The relation of the four important equations connecting the four important measured quantities (j, q, R_{ct}, C_{ct}) with the four PPI quantities (j_{inf}, q_{rev}, dj_{inf}/dE, dq_{rev}/dE)

	Kinetics	Coupling	Thermodynamics
AWV	$j = j_{inf} - H \cdot q$ Eq. (8)	$H = j_{inf}/q_{rev}$ Eq. (10)	$q = q_{rev} - (1/H) \cdot j$ Eq. (9)
dEIS	$\frac{1}{R_{ct}} = \frac{dj_{inf}}{dE} - \frac{dH}{dE} q$ Eq. (20)	$H = 1/(R_{ct} \cdot C_{ct})$ Eq. (22)	$C_{ct} = \frac{dq_{rev}}{dE} - \frac{d(1/H)}{dE} j$ Eq. (24)

There exist two usual complicating effect when we analyze voltametric curves: the IR drop, due to the non-zero solution resistance and the double layer charging. Both effects are – in principle – easy to be corrected following the ideas described in the context of diffusion-controlled charge transfer reactions [9]: if we measure high-frequency EIS and determine solution resistance R_s (at any potential) and double layer capacitance (as a function of potential). Since all potentials of this text are of interfacial nature, the IR drop must be subtracted from the applied potential; i.e. we have to plot j vs q points (and also the other point pairs of plots included in Table 1) corresponding to the same E–jR_s potential, and analyze these plots to extract j_{lim} and q_{rev}. The charging current error can be corrected if the double layer capacitance, C_{dl}, is also known from the high-frequency impedance measurements. As the charging current appears in the *rhs* of Eq. (1) as a $C_{dl}dE/dt$ term, one has to plot $j - C_{dl}dE/dt$ vs q instead of Equation (8), Actually, this is the point where the big advantage of dEIS is apparent over the traditional, simple AWV and EIS measurements: dEIS provides not only the information on kinetics (cf. Eq. 22) but simultaneously also the correction factors, R_s and C_{dl}.

The rate constant determination of the present paper is evidently much more correct than that of the widely used method, based on CV peak separation [10] (see also Ch. 14.3.3 of [1]). The superiority can be traced back to that complete CVs and/or multiple impedance spectra are evaluated together, rather than single (albeit characteristic) data points only.

The relations of the PPI functions of the present subject: j_{inf}, q_{rev} and their d/dE derivatives are summarized in Table 2. Three points are worth to be noted:

1. Information on kinetics and thermodynamics can be obtained from extrapolations to zero charge or to zero current, respectively, that is, to zero and to infinite time. Both the intercepts and the slopes of the linear equations of the dEIS are the potential derivatives of those of the AWV. This is how the large-signal and small-signal response functions (AWV and dEIS, respectively, of the given systems) are related to each other through their PPI forms.
2. The coupling constant H can be obtained from PPI functions calculated from AWV data; in contrast, from dEIS data one can calculate directly. This is why dEIS measurement is technically superior to AWV when the determination of rate coefficients is the goal.
3. The set of equations in Table 2 is analogous to that of the quasireversible diffusion-controlled redox reaction (see Table 2 of Ref. [3]). The differences are as follows: q (as $q(t)$ and q_{rev}) is to be replaced by M, the semi-integral of current density; H is a different combination of rate coefficients with diffusion coefficients and C_{ct} is to be replaced by σ_W, the Warburg admittance coefficient.

4 | CONCLUSIONS

The AWVs just as the Faraday-impedances obtained from dEIS of surface-confined redox species are complicated, scan-rate dependent curves with a hysteresis. By using the equations derived in this paper, one can transform these AWVs and the dEIS results to yield two independent potential functions of PPI forms for both methods. One of them is the charge transfer rate (or its potential derivate) as if the redox state of the surface were constant, whereas the other is the surface charge (or its potential derivate) as if there were steady-state at the given potential. This way it is possible to extrapolate to the purely kinetics-controlled and to the purely equilibrium-based situations.

The theory leading to the equations of Table 1 opens a new route for the data analyses related to the charge transfer rates of surface-confined redox reactions. Two practical advice are due here: (i) Use dEIS, and determine kinetics from the $R_{ct} \cdot C_{ct}$ products using also the correction factors, R_s and C_{dl}; (ii) Start the measurement from a potential well outside of the redox peak. Due to the algebraic analogies, the theory can be used also for evaluation of adsorption AWV and dEIS measurement results.

Two features of the theory bear special aesthetic value:

1. As $j_{inf}(E)$ and $q_{rev}(E)$ are the PPI forms of the large-signal response curves ("global" response functions) of the system. The $1/R_{ct,inf}(E)$ and $C_{ct,rev}(E)$ are the small signal, or "local" response functions. The local response functions are the potential derivatives of the global ones.
2. The connections between the measured quantities and the PPI functions, as summarized in Table 2, are surprisingly simple. The structure of the set of equations therein – *mutatis mutandis* – is just the same as in Table 2 of Ref. [4] that refers to diffusion-controlled charge transfer.

LIST OF SYMBOLS

t; E; v, j	time, electrode potential (in general), scan rate, current density
ε	electrode potential, in the context of Eqs. 5–10
Γ_A, q	surface concentration of the surface confined redox system, and its charge density
Γ_{ox}, Γ_{red}	surface concentration of the oxidized and reduced form of the redox system
$j_{inf}(E)$	limiting value of j at potential E if the redox system were completely reduced.
$q_{rev}(E)$	charge density at potential E in equilibrium state
k_{ox}, k_{red}	rate coefficient of the anodic and cathodic reactions
α_{ox}, α_{red}	charge transfer coefficient of the anodic and cathodic reactions
k_{ox}^0, k_{red}^0, E_0	standard rate coefficients and standard potential of the redox reaction
$H(E)$	parameter combination (sum) of k_{ox} and k_{red} (see Eq. 4.)
$R_{ct}(E)$	charge transfer resistance at potential E
$C_{ct}(E)$	pseudocapacitance associated with charge transfer at potential E
$R_{ct,inf}(E)$	limiting value of $R_{ct}(E)$ as if the redox system were completely reduced
$C_{ct,rev}(E)$	limiting value of $C_{ct}(E)$ in equilibrium state
E_{init}, q_{init}	initial (equilibrium) potential and charge density of the voltammetry measurement
$j_{inf}^{qinit}(E)$	$j_{inf}(E)$, if the initial charge of the redox system were q_{init}
$q_{rev}^{qinit}(E)$	$q_{rev}(E)$, if the initial charge of the redox system were q_{init}
$R_{ct,inf}^{qinit}(E)$	$R_{ct,inf}(E)$, if the initial charge of the redox system were q_{init}
$C_{ct,rev}^{qinit}(E)$	$C_{ct,rev}(E)$, if the initial charge of the redox system were q_{init}
n	charge number of the electrode reaction
F, R, T	Faraday's number, universal gas constant, temperature

DATA AVAILABILITY STATEMENT
Data available on request from the author.

ORCID
Tamás Pajkossy https://orcid.org/0000-0002-9516-9401

REFERENCES
1. K.B. Oldham, *Anal. Chem.* **1972**, *44*, 196.
2. T. Pajkossy, S. Vesztergom, *Electrochim. Acta* **2019**, *297*, 1121
3. T. Pajkossy, *Electrochim. Acta* **2019**, *308*, 410.
4. T. Pajkossy, *Electrochem. Comm.* **2020**, *118*, 106810.
5. A. J. Bard, L. R. Faulkner, *Electrochemical Methods*, 2nd ed. Wiley, Hoboken, NJ, **2001**
6. S. Srinivasan, E. Gileadi, *Electrochim. Acta* **1966**, *11*, 321.

7. J. C. Myland, K. B. Oldham, *Electrochem. Comm.* **2005**, *7*, 282
8. S. Trasatti, R. Parsons, *Pure & Appl.Chem.* **1986**, *58*, 437
9. J.C. Imbeaux, J.M. Savéant, *J. Electroanal. Chem.* **1973**, *44*, 169
10. E. Laviron, *J. Electroanal. Chem.* **1979**, *101*, 19

APPENDIX

Dependence of the PPI forms on E_{init}

In this Appendix, the derivation of Equations (8) to (11) and of Equations (20) to (24) is generalized for the case when the experiment starts from an arbitrary steady state E_{init} potential, where the electrode charge is $0 < q_{\text{init}} \le nF\Gamma_A$. This is done in two steps, as illustrated in Fig. 1d. In the first step, the potential is jumped or swept from a very negative potential to E_{init}, then we wait up till steady state is attained. Then, the following condition holds:

$$q_{\text{init}}(E_{\text{init}}) = q_{\text{rev}}(E_{\text{init}}) = j_{\text{inf}}(E_{\text{init}})/H(E_{\text{init}})$$

$$= nF \cdot \Gamma_A \cdot k_{\text{ox}}(E_{\text{init}})/H(E_{\text{init}}) \quad (27)$$

From the time of the potential program onward, irrespectively of the actual value of q_{init}, Equation (5) holds. Note that this $j(t)$ vs $q(t)$ function is linear, the slope, $-H(E)$, is the same as if q_{init} were zero as in Equation (6). Hence Equation (8) and (9) are to be modified by simply replacing the $q(t)$ terms to $q(t) + q_{\text{init}}$. The modified equations are as follows:

$$j(t) = j_{\text{inf}}(E) - H(E) \cdot q_{\text{init}} - H(E) \cdot q(t)$$

$$= j_{\text{inf}}^{\mathbf{qinit}}(E) - H(E) \cdot q(t) \quad (28)$$

$$q(t) = q_{\text{rev}}(E) - q_{\text{init}} - (1/H(E)) \cdot j(t)$$

$$= q_{\text{rev}}^{\text{qinit}}(E) - (1/H(E)) \cdot j(t) \quad (29)$$

The course of Eq. 28 is shown in Fig. A1. Here $j_{\text{inf}}^{\text{qinit}}(E)$ and $q_{\text{rev}}^{\text{qinit}}(E)$ are the modified ordinate intercepts. In what follows, the intercept-related quantities, for which $q_{\text{init}} > 0$, are denoted by the superscript "qinit."

As the slope of the $j(t)$ vs $q(t)$ line is $-H(E)$,

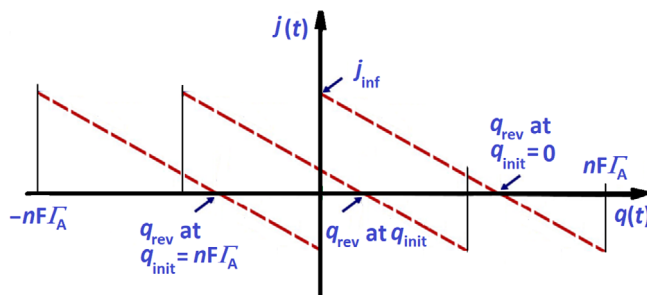$$q_{\text{rev}}^{\text{qinit}}(E) = j_{\text{inf}}^{\text{qinit}}(E)/H(E) \quad (30)$$

FIGURE A1   Illustration of how the characteristic line of Equation (28) shifts in negative direction with the positive shift of E_{init} (and q_{init}). Note that the slope is constant (as potential is constant) and the overall length of the line along the abscissa is $nF \cdot \Gamma_A$

Substituting the expressions of q_{init}, Equation (27), and $H(E_{\text{init}})$, Equation (4), into Equation (28) we get

$$j_{\text{inf}}^{\text{qinit}}(E)$$

$$= nF \cdot \Gamma_A \cdot \frac{k_{\text{ox}}(E) \cdot k_{\text{red}}(E_{\text{init}}) - k_{\text{red}}(E) \cdot k_{\text{ox}}(E_{\text{init}})}{k_{\text{ox}}(E_{\text{init}}) + k_{\text{red}}(E_{\text{init}})}$$

$$(31)$$

By combining Equations (30) and (31) we get

$$q_{\text{rev}}^{\mathbf{qinit}}(E) = \mathbf{n}F \cdot \Gamma_A$$

$$\cdot \frac{k_{\text{ox}}(E) \cdot k_{\text{red}}(E_{\text{init}}) - k_{\text{red}}(E) \cdot k_{\text{ox}}(E_{\text{init}})}{(k_{\text{ox}}(E) + k_{\text{red}}(E))(k_{\text{ox}}(E_{\text{init}}) + k_{\text{red}}(E_{\text{init}}))} \quad (32)$$

The impedance-related part of the theory can be generalized for the case of $q_{\text{init}} \ne 0$ in such a way that we start from Equation (5) and modify the Equations (16) and the ones onwards by replacing all $q(t)$ terms to $q(t) + q_{\text{init}}$. This way Equation (16) is written as

$$j(t) + \delta\mathbf{j} = nF \cdot \Gamma_A \cdot (k_{\text{ox}} + \delta k_{\text{ox}})$$

$$- (H + \delta\mathbf{H}) \cdot (q(t) + q_{\text{init}} + \delta\mathbf{q}) \quad (33)$$

Following the same line of thoughts as in the b section of the Theory we arrive at the expression of the Faradaic impedance:

$$Z(\omega) \equiv \overline{E_{\text{ac}}}/\overline{j_{\text{ac}}}$$

$$= \left(1 + \frac{H}{i\omega}\right) \bigg/ \left(\frac{dj_{\text{inf}}}{dE} - \frac{dH}{dE}(q(t) + q_{\text{init}})\right)$$

$$\equiv R_{\text{ct}}(E) + \frac{1}{i\omega C_{\text{ct}}(E)} \quad (34)$$

TABLE 3 The relation of the four important equations connecting the four important measured quantities (j, q, R_{ct}, C_{ct}) with the four PPI quantities (j_{inf}, q_{rev}, dj_{inf}/dE, dq_{rev}/dE) in the case when $q_{init} > 0$. Note that q_{init} does not appear in the C_{ct} - related equations

	Kinetics	Coupling	Thermodynamics
AWV	$j = j_{inf}^{qinit} - H \cdot q$ with $j_{inf}^{qinit} = j_{inf} - H \cdot q_{init}$ Eq. (28)	$H = j_{inf}^{qinit}/q_{rev}^{qinit}$ Eq. (35)	$q = q_{rev}^{qinit} - (1/H) \cdot j$ with $q_{rev}^{qinit} = q_{rev} - q_{init}$ Eq. (29)
dEIS	$\frac{1}{R_{ct}} = \frac{1}{R_{ct,inf}^{qinit}} - \frac{dH}{dE} \cdot q$ with $\frac{1}{R_{ct,inf}^{qinit}} = \frac{dj_{inf}}{dE} - \frac{dH}{dE} q_{init}$ Eq. (36)	$H = 1/(R_{ct} \cdot C_{ct})$ Eq. (35)	$C_{ct} = C_{ct,rev}^{qinit} - \frac{d(1/H)}{dE} j$ with $C_{ct,rev}^{qinit} =$ $C_{ct,rev} = \frac{dq_{rev}}{dE}$ Eq. (39)

Equation (19) expresses the impedance of a charge transfer resistance, R_{ct}, and an associated pseudocapacitance, C_{ct}, connected serially. Their values are coupled to each other as

$$R_{ct}(E) \cdot C_{ct}(E) = \mathbf{H}(E) \quad (35)$$

holds for any $q(t)$ and q_{init}. These elements are as follows:

$$\frac{1}{R_{ct}(E)} = \frac{dj_{inf}}{dE} - \frac{dH}{dE} q_{init} - \frac{dH}{dE} q(t)$$

$$= \frac{1}{R_{ct,inf}^{qinit}(E)} - \frac{dH}{dE} q(t) \quad (36)$$

$$C_{ct}(E) = \frac{1}{H} \cdot \left(\frac{dj_{inf}}{dE} - \frac{dH}{dE} q_{init} \right) - \frac{1}{H} \cdot \frac{dH}{dE} q(t) \quad (37)$$

For $1/R_{ct}$ and C_{ct} both, a $const_1 - const_2 \times q$ type equation applies where the constants are related also to the constants of the *dc* relations:

The $q(t)$ function is replaced by $j(t)$ using Equation (29), and j_{inf} is expressed by q_{rev} using Equation (10). This way, Equation (36) is transformed to

$$\frac{1}{R_{ct}(E)} = \frac{dj_{inf}}{dE} - \frac{dH}{dE} q(t) - \frac{dH}{dE} q_{init} =$$

$$= \frac{d(H \cdot q_{rev})}{dE} - \frac{dH}{dE} \left(q_{rev}(E) - q_{init} - \frac{1}{H(E)} \cdot j(t) \right)$$

$$- \frac{dH}{dE} q_{init} = H \cdot \frac{dq_{rev}}{dE} + \frac{1}{H} \cdot \frac{dH}{dE} j(t) \quad (38)$$

For the C_{ct} vs j equation, we combine Equations (35) and (38) to yield

$$C_{ct}(E) = \frac{1}{H(E) \cdot R_{ct}(E)} = \frac{dq_{rev}}{dE} + \frac{1}{H^2} \cdot \frac{dH}{dE} j(t)$$

$$= C_{ct,rev}(E) - \frac{d(1/H)}{dE} j(t) \quad (39)$$

Note that q_{init} does not appear in Equations (38) and (39). As it is shown in Table 3, all but one intercepts

depend on the q_{init}. ($C_{ct,rev}^{qinit}$ is the exception, because it would depend on the potential derivative of a constant (q_{init}).

Note that up till here, no functional form of $k_{ox}(E)$ and $k_{red}(E)$ has been specified; a trivial assumption is that $k_{ox}(E)$ is small at negative and large at positive potentials; for $k_{red}(E)$ just the opposite trends apply. For j_{inf}^{qinit} and q_{rev}^{qinit} we have the complicated Equations (31) and (32). They can be simplified only if exponential potential dependences are assumed, i.e. $k_{ox}(E) = k_{ox}^0 \cdot \exp(\alpha_{ox} FE/RT)$ and $k_{red}(E) = k_{red}^0 \cdot \exp(-\alpha_{red} FE)/RT)$. With these dependencies Equation (31) changes to

$$j_{inf}^{qinit}(E) = nF\Gamma_A \cdot \frac{k_{red}(E_{init}) \cdot k_{ox}(E_{init})}{k_{ox}(E_{init}) + k_{red}(E_{init})}$$

$$\cdot [\exp(\alpha_{ox} F(E - E_{init})/RT) - \exp(-\alpha_{red} F(E - E_{init})/RT)]$$

$$(40)$$

This is the generalized form of Equation (12). Note that Equation (40) is of the same form as the Butler-Volmer equation.

For obtaining $q_{rev}^{qinit}(E)$, consider Equation (29). According to it, $q_{rev}^{qinit}(E) = q_{rev}(E) - q_{init}$. The second term of the *rhs* is a constant, the first term has already been analyzed in the voltammetry theory section, cf. Equations (12) and (13), leading to the sigmoid-shape curve of Equations (14) and (15). Because of the $-q_{init}$ term, this sigmoid-shape curve gets shifted in negative direction with q_{init}, and the equations have the following form:

$$q_{rev}^{qinit}(E) = (nF \cdot \Gamma_A/2) \cdot [1 + \tanh(nF(E - E_0)/RT)]$$

$$- q_{rev}(E_{init}) \quad (41)$$

and

$$\mathbf{E} = E_0 + \frac{RT}{nF} \ln \left[\frac{q_{rev}^{qinit}(E) - q_{rev}(E_{init})}{nF \cdot \Gamma_A - q_{rev}^{qinit}(E)} \right] \quad (42)$$

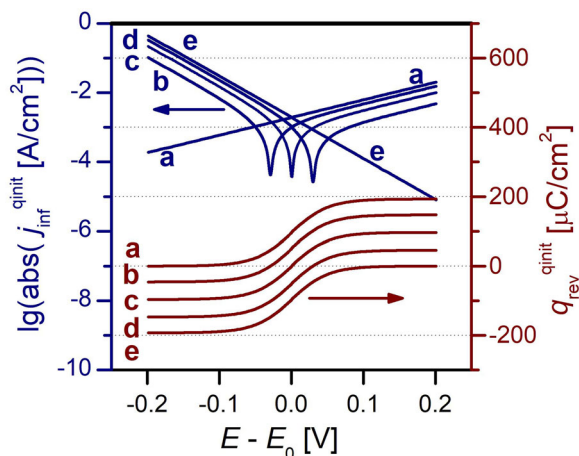Equations (41) and (42) are the general forms of Equations (14) and (15).

FIGURE A2 PPI forms of the CVs of the system of Figure 3, with E_{init} -1 V (a), -0.03 V(b), 0 V (c), +0.3 V (d), and +1 V (e)

There are two, simple, trivial special cases of Equations (40) and (41):

First, when $E_{init} - E_0$ is sufficiently negative (typically, when the difference exceeds a few hundred mV) then

$$j_{inf}^{qinit} = j_{inf} = nF \cdot \Gamma_A \cdot k_{ox}^0 \cdot \exp\left(\alpha_{ox} FE/RT\right)$$

and

$$q_{rev}^{qinit} = q_{rev} = (nF\Gamma_A/2) \cdot [1 + \tanh\left(nF(E - E_0)/RT\right)] \tag{43}$$

Second, for sufficiently positive $E_{init} - E_0$,

$$j_{inf}^{qinit}(E) = -nF \cdot \Gamma_A \cdot k_{red}^0 \cdot \exp\left(-\alpha_{red} FE\right)/RT)$$

and

$$q_{rev}^{qinit} = q_{rev} - nF\,\Gamma_A$$
$$= (nF\Gamma_A/2) \cdot [-1 + \tanh\left(nF(E - E_0)/RT\right)]. \tag{44}$$

The j_{inf}^{qinit} vs E and the q_{rev}^{qinit} vs E dependencies are illustrated in Figure A2. for various E_{init} initial potentials. Note that the "simple" curves (a and e) are the ones when the voltammetry experiment started from potentials where the redox system is either fully reduced or fully oxidized (cf. Equations (43) and (44)). Hence a practical suggestion: start the measurements with either completely reduced or completely oxidized redox system on the surface.